第33卷第4期 2014年8月 | 红外与毫米波学报 J. Infrared Millim. Waves | Vol. 33, No. 4 August, 2014

文章编号:1001-9014(2014)04-0333-04 DOI:10.3724/SP.J.1010.2014.00333

Performance of InGaAs detector with SiN diffusion mask

WANG Yun-Ji[1,2,3], TANG Heng-Jing[1,2], LI Xue[1,2], SHAO Xiu-Mei[1,2], YANG Bo[1,2], DENG Shuang-Yan[1,2], GONG Hai-Mei[1*]

(1. State Key Laboratories of Transducer Technology, Shanghai Institute of Technical Physics, Chinese Academy of Sciences, Shanghai 200083, China;
2. Key Laboratory of Infrared Imaging Materials and Detectors, Shanghai Institute of Technical Physics, Chinese Academy of Sciences, Shanghai 200083, China;
3. University of Chinese Academy of Sciences, Beijing 100039, China)

Abstract: The InGaAs planar detectors with SiN_x film as diffusion mask were fabricated SiNx films were grown by plasma enhanced chemical vapor deposition (PECVD) or by low temperature ICP-CVD inductively coupled plasma chemical vapor deposition (ICP-CVD). The photoelectric responses of the detectors made with the two methods were investigated. It turns out that the two kinds of devices have similar performance in the average response rate 0.73 and 0.78 A/W, the average peak detectivity 6.20E11 and 6.32E11 $cmHz^{1/2}W^{-1}$, and the quantum efficiency 56.0% and 62.0%, respectively. However, the average dark current densities of the detectors is much different, with the values of 312.9 nA/cm^2 and 206 nA/cm^2 (−0.1 V), respectively. By fitting with experimental data to electrical transport theory, the mechanism of dark current was analyzed. The results indicate that the device using SiN_x deposited by ICP-CVD has reduced ohmic dark current in comparison with devices with SiN_x deposited by PECVD.

Key words: InGaAs, ICP-CVD, diffusion mask, dark current
PACS: 85.60.Gz

不同扩散掩膜方式对InGaAs平面探测器性能影响研究

王云姬[1,2,3], 唐恒敬[1,2], 李 雪[1,2], 邵秀梅[1,2], 杨 波[1,2], 邓双燕[1,2], 龚海梅[1*]

(1. 中国科学院上海技术物理研究所 传感技术国家重点实验室,上海 200083;
2. 中国科学院上海技术物理研究所 红外成像材料和器件重点实验室,上海 200083;
3. 中国科学院大学,北京 100039)

摘要:测量了不同扩散掩膜生长方式的截止波长为1.70 μm的InGaAs平面探测器的电学性能.其中,SiN_x薄膜作为扩散掩膜,分别采用等离子体化学气相沉积(PECVD)和低温诱导耦合等离子体化学气相沉积(ICP-CVD)生长.探测器焊接在杜瓦里测量,结果显示采用两种掩膜方式的器件的平均峰值响应率、探测率和量子效率分别为0.73和0.78 A/W,6.20E11和6.32E11$cmHz^{1/2}W^{-1}$,56.0%和62.0%;两种器件的响应波段分别为1.63~1.68 μm和1.62~1.69 μm;平均暗电流密度分别为312.9 nA/cm^2和206 nA/cm^2.通过理论分析两种器件的暗电流成分,结果显示,相对于采用PECVD作为扩散掩膜生长方式而言,采用ICP-CVD作为扩散掩膜生长方式大大降低了器件的欧姆暗电流成分.

关 键 词:InGaAs;诱导耦合等离子体化学气相沉积(ICP-CVD);扩散掩膜;暗电流

中图分类号:TN215 **文献标识码**:A

Received date: 2013-12-11, **revised date**: 2014-06-13 **收稿日期**:2013-12-11, **修回日期**:2014-06-13

Foundation items: Supported by National Key Basic Research and Development Program of China (2012CB619200), the Key Program of the National Natural Science Foundation of China (61205105, 61007067, 61376052).

Biography: WANG Yun-Ji, (1987-), female, Shanghai, Ph. D. candidate. Research area is SWIR detector. E-mail: wangyun_ji@126.com

* **Corresponding author**: E-mail: hmgong@mail.sitp.ac.cn

Introduction

The ternary InGaAs has advantages of material growth, device process technology, and better performance of the photodiodes at higher operation temperature[1]. After decades of development, InGaAs detectors, including linear and large-scale InGaAs detectors arrays, have acquired wide applications in many fields such as near-infrared spectroscopy, earth environmental resource research, thermal imaging, night vision and space remote sensing[2-5].

The planar type InGaAs detectors have attracted particular attention due to the higher reliability and lower dark current[6-7]. To fabricate the planar type InGaAs detector, doping concentration and the quality of the p-n junction are directly related to the performance of the device, so the diffusion process is very important in device fabrication. The high-temperature-deposited SiN_x film grown by PECVD is usually used as the diffusion mask [8]. However, to the best of our knowledge, no studies have been reported on the effect of low-temperature-deposited SiN_x grown by ICP-CVD which is used as diffusion mask and its direct impact on the photodiode characteristics. This work compared the behavior of $In_{0.53}Ga_{0.47}As$ photodiodes with that using SiN_x as diffusion mask grown by PECVD with that by ICP-CVD, respectively.

1 Experimental

The planar-type back-illuminated photo detectors were fabricated on n-InP/i-InGaAs/n-InP epitaxial materials. The epitaxial structure consisted of 1 μm n-InP top layer with a carrier concentration of 5×10^{16} cm^{-3}, a 2.5 μm i-InGaAs absorbing layer with a carrier concentration of 5×10^{16} cm^{-3}, a 0.5 μm n-InP buffer layer with a carrier concentration of 2×10^{18} cm^{-3} and a 650 μm n-InP substrate with a carrier concentration of 7×10^{18} cm^{-3}. 0.23 μm thick SiN_x was deposited on the surface as the diffusion mask by means of PECVD (330℃) and ICP-CVD (75℃), respectively. The detector was obtained by a series of planar fabrication processes such as sealed-ampoule diffusion, photolithography, SiN_x passivation and growth of electrode. The detectors are in an array of 32 × 32 scale with a designed photosensitive area size of 30 μm × 30 μm, as show in Fig. 1, the detectors with different diffusion masks are marked as Sample-1 and Sample-2, respectively.

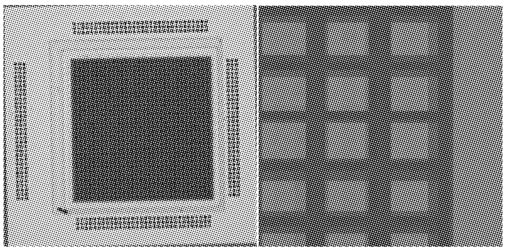

Fig. 1 The photograph of the detectors
图1 探测器的显微照片图

2 Results and discussions

As shown in Table 1, the average peak response rate of the two detectors are 0.73 and 0.78 A/W, the average peak detectivity are 6.20E11 and 6.32E11 cmHz$^{1/2}$W^{-1}.

Table 1 R_p and D_p of sample-1 and sample-2
表1 样品一和样品二的 R_p 和 D_p

Number	R_p/(A/W)	D_p/(cmHz$^{1/2}$W^{-1})
Sample-1	0.73	6.20E11
Sample-2	0.78	6.32E11

Quantum efficiencies were calculated as follows

$$\eta_1 = \frac{R_{\lambda_p}}{0.8\times\lambda_p} = \frac{0.73}{0.8\times1.63} = 56.0\% \quad ,(1)$$

$$\eta_2 = \frac{R_{\lambda_p}}{0.8\times\lambda_p} = \frac{0.78}{0.8\times1.62} = 60.2\% \quad .(2)$$

As shown in Fig. 2, the response wavelength of the two devices is in the range of 1.63 ~ 1.68 μm and 1.62 ~ 1.69 μm, respectively. It can be concluded that the optical performance of the photodiodes with SiN_x as diffusion mask deposited by ICP-CVD are improved than the photodiodes with SiN_x deposited by PECVD.

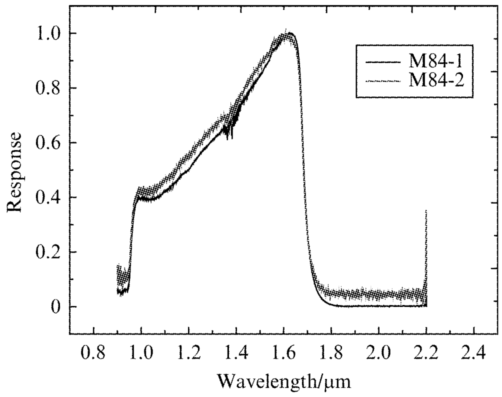

Fig. 2 The spectral response of sample-1 and sample-2
图2 样品1和样品2的响应光谱图

The characteristics of the detectors were studied by *I-V* curves. Figure. 3 shows the *I-V* plots of Sample-1 and Sample-2. As shown in table 2, the average dark current densities of Sample-1 and Sample-2 is 312.9 nA/cm^2 and 206 nA/cm^2 (−0.1 V), and the figure of merit R_oA are 1.85×10^5 Ω. cm^2 and 2.24×10^5 Ω. cm^2, respectively. The dark current density of photodiodes with SiN_x as diffusion mask formed by ICPCVD has been reduced about 30% off, as shown in Fig. 3, and the R_oA has been increased.

The current flowing through the diode is low without the light illumination; *I-V* relationship of the device can be expressed as

$$I = I_0\left[\exp\left(\frac{qV}{nKT}-1\right)\right] \quad . \quad (3)$$

The above formula can be transformed into In*I* =

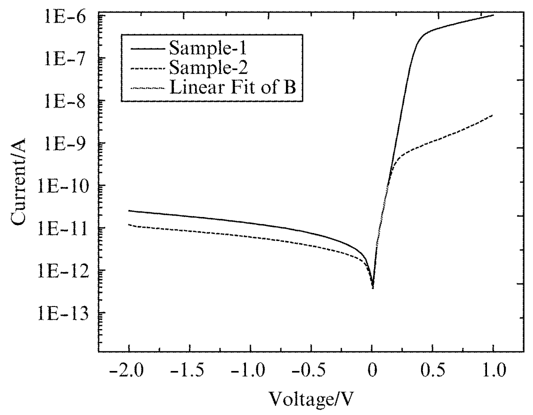

Fig. 3 The *I-V* curves of Sample-1 and Sample-2
图 3 Sample-1 和 Sample-2 的 *I-V* 曲线

Table 2 Dark current density J_d (−0.1 V) and figure of merit R_0A of Sample-1 and Sample-2
表 2 负 0.1 V 下两种样品的暗电流密度和优值因子

Number	J_d/(nA/cm^2)	R_0A/(Ω. cm^2)
Sample-1	312.9	1.85E5
Sample-2	206	2.24E5

$\ln I_0 + \left(\frac{q}{nKT}\right)V$. Where I_0 is reverse saturation current, T is temperature of detector, k is Boltzman constant, V is voltage, n is ideality factor limited by current mechanism. The ideality factor n can be obtained by fitting the linear part of the ln*I-V* curve.

By fitting the dark current at small forward bias, the ideality factors n of Sample-1 and Sample-2 are obtained 1.09 and 1.15, respectively. The results indicate that at small forward bias, the dark current of the device is dominated by diffusion dark current. For Sample-1, in the range of small forward bias (0.04 ~ 0.22 V), the experimental results were fitted with as, the diffusion dark current shown in Fig. 4 and expressed as

$$I_{diff} = 4.68992 \times 10^{-3} \times \left(\exp\left(\frac{V}{0.026}\right) - 1\right) \quad . (4)$$

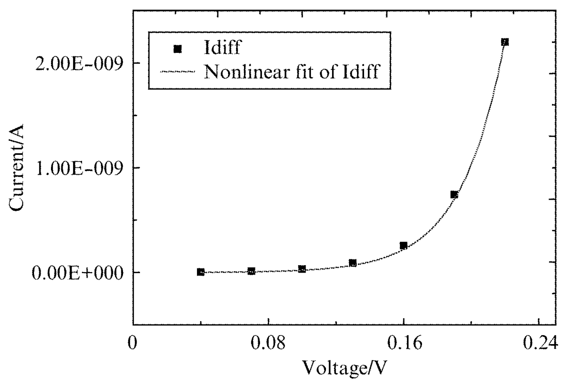

Fig. 4 The nonlinear fitting of sample-1 at the small forward bias
图 4 Sample-1 正向小偏压下的非线性拟合

The dark current at the reverse bias were fitted by the sum of diffusion, generation and recombination, ohmic component, as shown in Fig. 5. These components, in addition to the diffusion one shown in Eq. 4 can be expressed separately as

$$I_{gr} = 1.66909 \times 10^{-12} \times \sqrt{0.65 - V} \times \left(\exp\left(\frac{V}{0.552}\right) - 1\right) \quad , (5)$$

$$I_{sh} = 1.02566 \times 10^{-11} \times V \quad . (6)$$

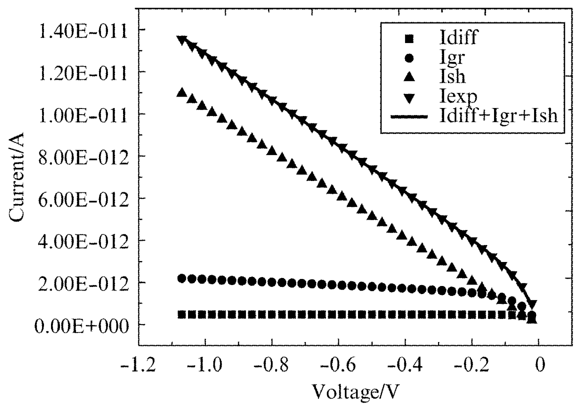

Fig. 5 The different dark current components of Sample-1
图 5 Sample-1 的不同暗电流成分

In the same way, as shown in Fig. 6, the dark current component at reverse bias for Sample-2 is presented as follows

$$I_{diff} = 6.18095 \times 10^{-13} \times \left(\exp\left(\frac{V}{0.026}\right) - 1\right) \quad , (7)$$

$$I_{gr} = 1.00557 \times 10^{-12} \times \sqrt{0.65 - V} \times \left(\exp\left(\frac{V}{0.052}\right) - 1\right) \quad , (8)$$

$$I_{sh} = 4.14396 \times 10^{-12} \times V \quad . (9)$$

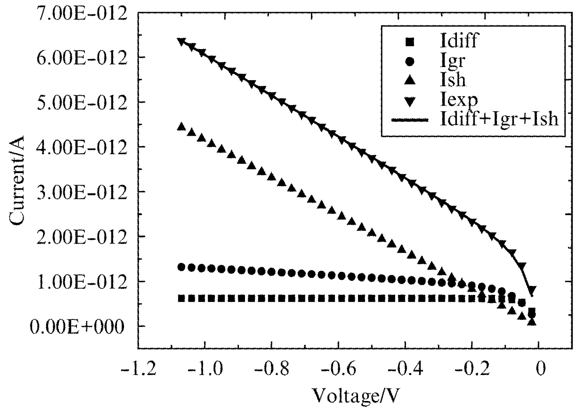

Fig. 6 The different dark current components of Sample-2
图 6 Sample-2 的不同暗电流成分

Comparing the dark current components of the two devices at reverse bias in Fig. 7, it can be concluded that the ohmic component of the dark current is reduced in the devices with SiN_x deposited by ICP-CVD.

3 Conclusions

The InGaAs planar detectors using SiN_x as diffusion mask deposited by PECVD and ICP-CVD have been

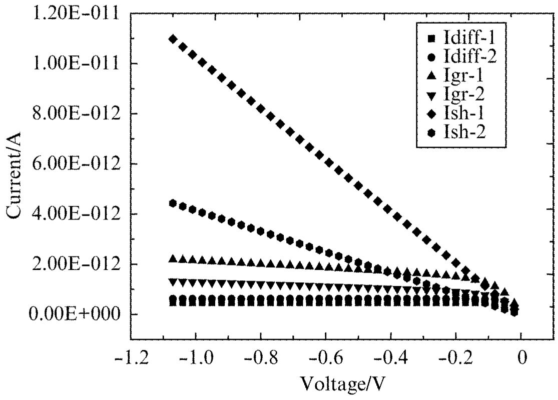

Fig. 7 The different dark current components of Sample-1 and Sample-2

图7 Sample-1 和 Sample-2 的不同暗电流成分比较

fabricated. Impact of different fabrication process on the performance of the detectors was studied. The average dark current density of the detector using SiN_x as diffusion mask deposited by ICP-CVD is 206 nA/cm^2 (−0.1 V), nearly 30% off in comparing with 312.9 nA/cm^2, that of deposited by PECVD. Dark current analysis reveals that the device with SiN_x formed by ICPCVD has a small ohmic current component.

References

[1] Rouvie A, Huet Q. SWIR InGaAs focal plane arrays in France[J]. *Proc. SPIE*, 2013, **8704**: 870403.

[2] Cohen M J, Olsen G H. Room temperature camera for NIR imaging [J]. *Proc. SPIE*, 1993, **1946**: 436 −443.

[3] Li Y F, Tang H J, Li T, *et al.* Suppression of extension of the photosensitive area for a planar-type front-illuminated InGaAs detector by the LBIC technique[J], *J. Semicond*, 2010, **31**(1): 013002 −1 −5.

[4] Joshi A M, Ban V S, Mason S, *et al.* 512 and 1024 element linear InGaAs detector arrays for near infrared (1 ~3 μm) environmental sensing [J], *Proc SPIE*, 1992, **1735**: 287.

[5] Kozlowski L J, Tennant WE, Zandian M, *et al.* SWIR staring FPA performance at room temperature[J], *Proc SPIE*, 1996, **2746**: 93.

[6] Hoogeveen R W M, van der Ronald J A, Goede A P H. Extended wavelength In GaAs infrared(1.0 ~2.0 μm) detector arrays on SCIAMACHY for space-based spectrometry of the Earth atmosphere[J], *Infrared Physics & Technology*, 2001, **42**: 1

[7] Yuan Y, Meixell M. Low dark current small pixel large format InGaAs 2D photodetector array development at Teledyne Judson technologies [J]. *Proc. SPIE*, 2012, **8353**: 835309.

[8] Onat B M, Huang W, Masaun N, *et al.* Ultra low dark current InGaAs technology for focal plane arrays for low-light level visible-shortwave infrared imaging[J]. *Proc. SPIE*, 2007, **6542**: 65420L.